

Supporting Information

for

Amine Decorated Polystyrene Nanobeads Incorporating π -Conjugated OPV Chromophore for Picric acid Sensing in Water

Sarabjot Kaur Makkad^{a, b}

- a) Govt. Autonomous NPG College of Science, Raipur, India.
- b) CSIR-National Chemical Laboratory, Pune , India.

Table of Content

Section	Subject	Page No
Table S1	Number and weight average molar mass, polydispersity indices (PDI), solid content, zeta potential of PS-OPV-NH ₂ .	S4
Table S2	Dye loading content (DLC), Dye loading efficiency (DLE), polydispersity index (D).	S4
Table S3	Average quenching percentage of OPV emission and quenching \pm error (%) after the addition of the respective nitro compounds in water.	S4
Table S4	Average quenching percentage of OPV emission and quenching \pm error (%) after the addition of the anions in water.	S5
Table S5	Average quenching percentage of OPV emission and quenching \pm error (%) after the addition of the cations in water.	S6
Table S6	Comparison table for fluorescent sensors of PA in the literature.	S7
Scheme S1	Chemical structures of nitro-organic compounds.	S8
Figure S1	FTIR plot of polymer on KBr pellet.	S8
Figure S2	Normalized intensity-average size distribution of polymer in demineralized water using Dynamic Light Scattering.	S8
Figure S3	TEM image of PS-OPV-NH ₂ polymer.	S9
Figure S4	Absorption spectra of the polymer in THF (1mg/ml) for DLC and DLE calculation.	S9
Figure S5	Solution state (a) emission and (b) excitation spectra of the polymer PS-OPV-NH ₂ in demineralized water.	S9
Figure S6	CIE co-ordinate diagram of PS-OPV-NH ₂ .	S10
Figure S7	Emission spectra for PS-OPV-NH ₂ depicting non-quenching of OPV emission on varying pH from 1 to 14.	S10
Figure S8	Emission spectra for PS-OPV-NH ₂ depicting non-quenching of OPV emission on varying temperature from 0°C to 60°C.	S10
Figure S9.	Plot of linear ranges using Stern-Volmer equation from 0 to 30 ($R^2 = 0.982$) and 40 to 70 μ M ($R^2 = 0.998$).	S11
Figure S10	Plot of absorption spectra of PS-OPV-NH ₂ on varying concentration of PA.	S11

Figure S11	Mechanism of quenching depicting the overlap of absorption spectra of nitrophenols to that of OPV emission.	S11
Figure S12	Emission spectra of PS-OPV-NH ₂ after the addition of 1M NaCl.	S12
Figure S13	Quenching observed on dipping free standing film into PA in water.	S12
	References	S12

Table S1. Number and weight average molar mass, polydispersity indices (PDI), solid content, zeta potential of PS-OPV-NH2.

Sample	Mn ^a	Mw ^a	PDI ^a (D)	Solid content (%)	Zeta Potential ^b
PS-OPV-NH2	56700	151000	2.6	21	+36.6

- a) Measured by Gel Permeation Chromatography (GPC) in Chloroform (CHCl_3) calibrated with linear, narrow molecular weight distribution polystyrene standards.
- b) Measured by Dynamic Light Scattering in water.

Table S2. Dye loading content (DLC), Dye loading efficiency (DLE), polydispersity index (D).

Sample	Amount of OPV in feed (mg)	Amount of OPV incorporated (mg) ^a	DLC (%) ^a For OPV	DLE (%) ^a For OPV	Size (nm) ^b	PDI ^b
PS-OPV-NH2	30	16.1	1.6	53.6	182	0.08

- a) Dye Loading content (DLC) and Dye Loading Efficiency (DLE) are calculated by absorption studies in THF.
- b) Measured by Dynamic Light Scattering in water.

Table S3. Average quenching percentage of OPV emission and quenching \pm error (%) after the addition of the respective nitro compounds in water.

Nitro compounds	Average Quenching (%)	Quenching \pm Error (%)
Ph	6.8	0.4
1,2-DCB	7.1	0.5
4-NBA	7.4	0.5
BA	7.7	0.7

1,5-DNN	8.6	1.2
2,4-DNT	9.6	0.5
4-HBA	8.1	1.5
4-NT	9.6	1.8
NM	9.5	2.5
1,4-DNB	20.4	1.2
2-NP	34.3	1.1
2,4-DNP	71.3	1.9
PA	91.5	1.5

Table S4. Average quenching percentage of OPV emission and quenching ± error (%) after the addition of the anions in water.

Nitro compounds	Average Quenching (%)	Quenching ± Error (%)
NO ₂ ⁻	2.3	0.3
SO ₄ ²⁻	2.7	0.6
Cl ⁻	3.4	0.8
Br ⁻	3.7	1.3
NO ₃ ⁻	4.1	1.9
AcO ⁻	4.2	1.4
SO ₃ ²⁻	5.1	0.8
HPO ₄ ⁻	5.7	1.3
F ⁻	5.9	0.8
I ⁻	8.1	0.4
PA	91.5	1.5

Table S5. Average quenching percentage of OPV emission and quenching \pm error (%) after the addition of the cations in water.

Nitro compounds	Average Quenching (%)	Quenching \pm Error (%)
Hg(II)	2.3	0.3
Cu(II)	2.4	0.3
Fe(II)	2.7	0.6
Pb(I)	2.7	0.5
K(I)	3.1	0.9
Ni(II)	3.2	1.6
Cr(III)	3.3	1.2
Ca(II)	3.3	1.1
Na(I)	3.4	0.8
Co(II)	3.5	2.1
Mn(II)	3.9	1.7
Zn(II)	4.0	0.5
Cd(II)	4.8	1.3
Al(III)	5.4	0.9
Cs(I)	5.9	0.8
Fe(III)	9.3	0.7
PA	91.5	1.5

Table S6. Comparison table for fluorescent sensors of PA in the literature.

Material	Linear Range (μM)	LOD	Medium Used	Interference from cations and anions	Effect of pH	Selectivity	Ref.
Metal organic framework	-	-	Acetonitrile	Not Checked	-	Yes	S1
Organic Cage	-	0.06 μM (6.4 ppb)	Dichloromethane (DCM)	Not Checked	-	Yes	S2
Small molecules	0-10	0.5 μM	Ethanol	Not Checked	-	Poor	S3
Small molecules	2-16	2 μM	DMSO-Chloroform	Not Checked	-	Poor	S4
Small molecules	0-20	0.35 μM	Toluene-DCM	Not Checked	-	Poor	S5
Metal organic framework	0-50	2.5 μM	Dimethyl acetamide (DMA)	Not Checked	-	Yes	S6
Covalent organic polymer	-	4.37 μM	Methanol	Not Checked	-	Yes	S7
Small molecules	0-1	.28 μM	Water/ THF (7:3)	No interference	-	Yes	S8
Tetraphenyl ethylene Nanosphere	-	0.005 μM	Water/ THF (9:1)	Not Checked		Yes	S9
Iridium complex	-	-	Water/acetone (9:1)	Slightly for Hg(II)	No effect	Yes	S10
Conjugated polyelectrolytes	0-51	0.72 μM	Water/ THF (9:1)	Not Checked	-	Not studied	S11
Inorganic polymer	-	(54 $\mu\text{g/mL}$) 1ppm	Water/ THF (9:1)	Not Checked	-	Not studied	S12
Hyperbranched polymer	-	1 $\mu\text{g/mL}$	Water/ THF (9:1)	Not Checked	-	Not studied	S13
Functional polymer		1 μM	Water/ THF (9:1)	Not Checked	-	Non-selective	S14
MoS ₂ Quantum dots	0.99-36.5	0.095	Water	Moderate interference from Fe(III), Ni(II), Hg(II), Co (II)	-	Yes	S15
Conjugated polyelectrolytes	0-20	128 ppt	Water	Not Checked	-	Yes	S16
Graphene oxide	-	0.55 μM	Water	Not Checked	-	Yes	S17
Small molecules	0.01-0.07	0.013 μM	Water	No interference	-	Yes	S18
Carbon dots	-	0.10 μM	Water	Moderate interference observed	pH dependent quenching	Yes	S19
Carbon dots	-	1 μM	Water	Not Checked	pH dependent quenching	Yes	S20
Non conjugated polymer NPs	0.05-70	0.026 μM	Water	Appreciable interference from Cu(II), Ni(II), Fe(III), Zn(II)	pH dependent quenching	Yes	S21
PS nanobeads	0-30; 40-70	0.058 μM	Water	No interference at all	No dependence	Yes	This work

Scheme S1. Chemical structures of nitro-organic compounds.

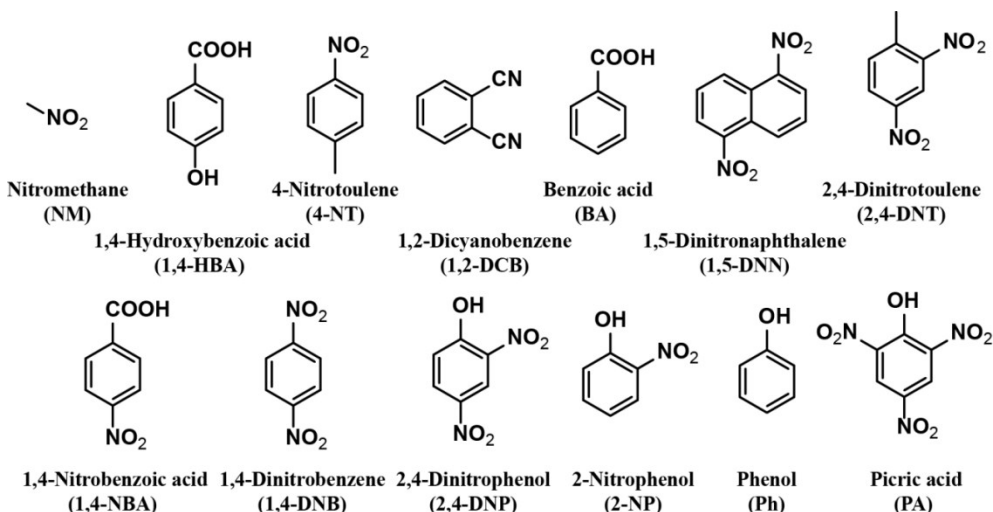


Figure S1. FTIR plot of polymer on KBr pellet.

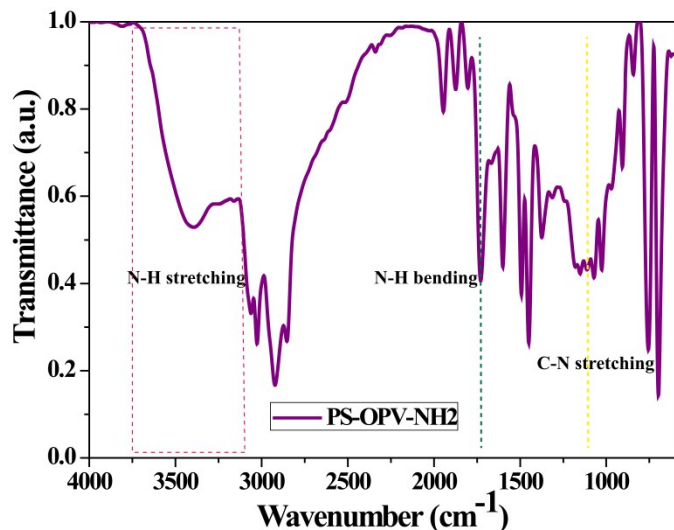


Figure S2. Normalized intensity-average size distribution of polymer in demineralized water using Dynamic Light Scattering.

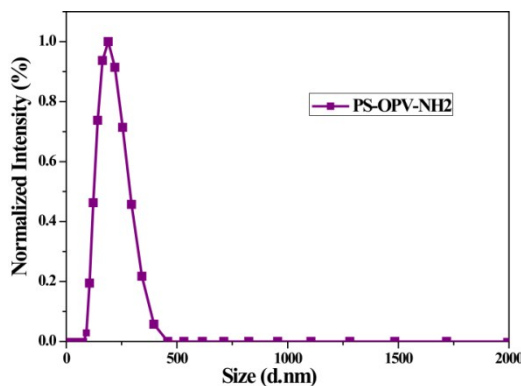


Figure S3. TEM image of PS-OPV-NH₂ polymer.

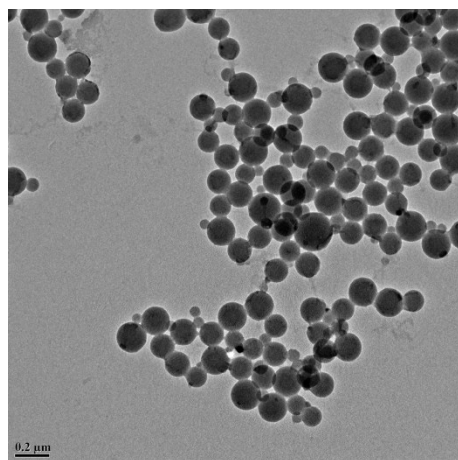


Figure S4. Absorption spectra of the polymer in THF (1mg/ml) for DLC and DLE calculation.

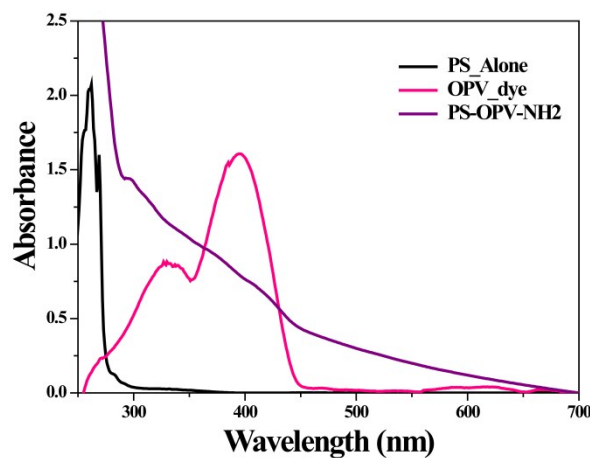


Figure S5. Solution state (a) emission (at 390 nm) and (b) excitation spectra (collected at 445 nm) of the polymer PS-OPV-NH₂ in demineralized water.

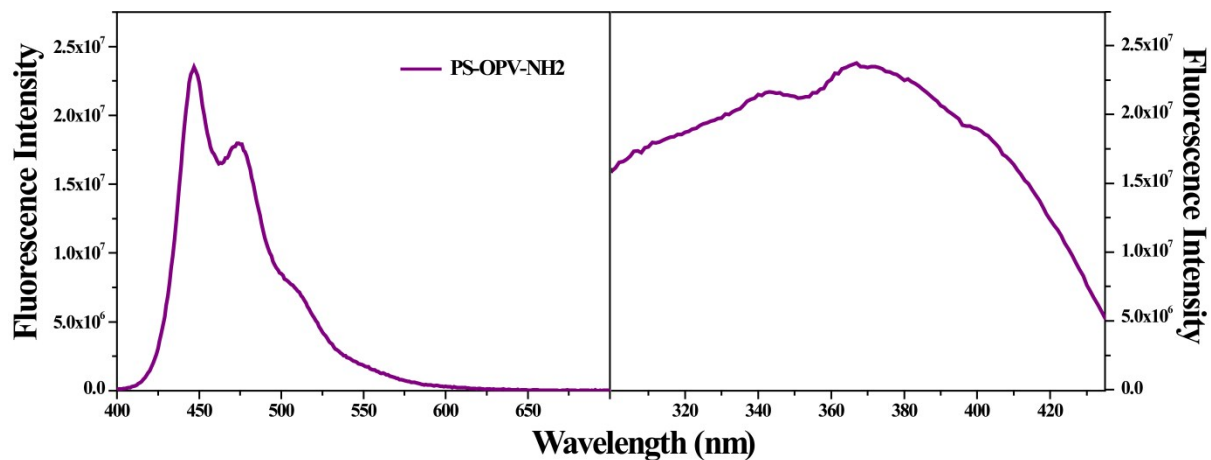


Figure S6. CIE co-ordinate diagram of PS-OPV-NH2.

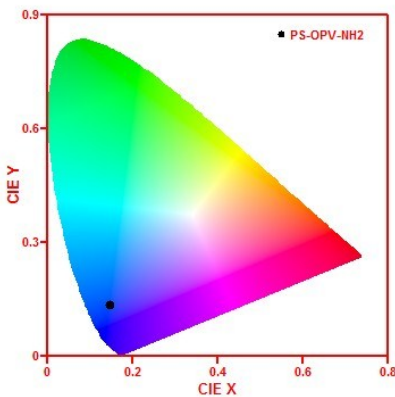


Figure S7. Emission spectra for PS-OPV-NH2 depicting non-quenching of OPV emission on varying pH from 1 to 14.

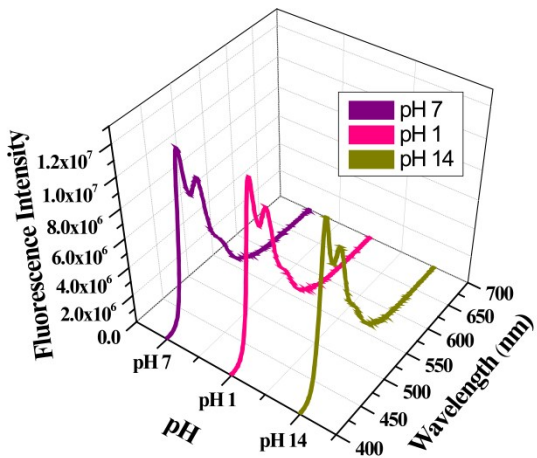


Figure S8. Emission spectra for PS-OPV-NH2 depicting non-quenching of OPV emission on varying temperature from 0°C to 60°C.

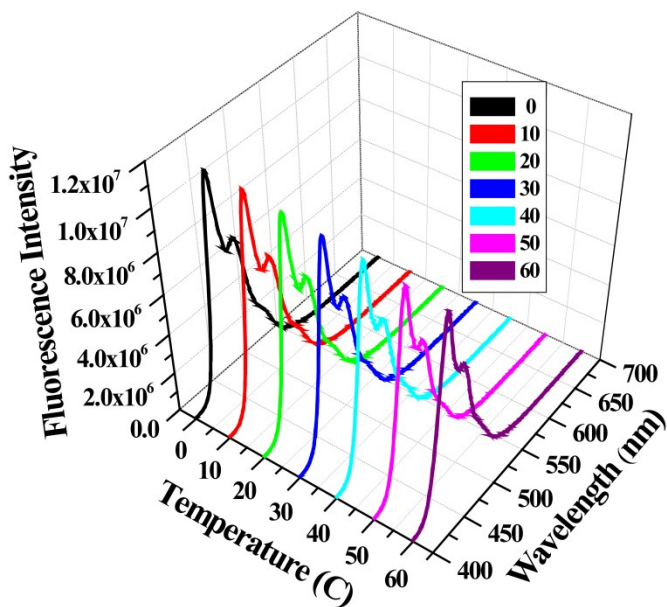


Figure S9. Plot of linear ranges using Stern-Volmer equation from 0 to 30 ($R^2 = 0.982$) and 40 to 70 μM ($R^2 = 0.998$).

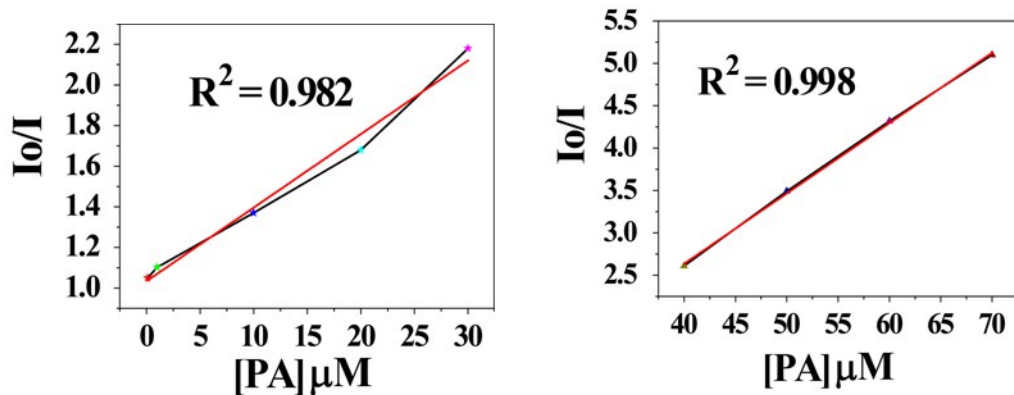


Figure S10. Plot of absorption spectra of PS-OPV-NH₂ on varying concentration of PA.

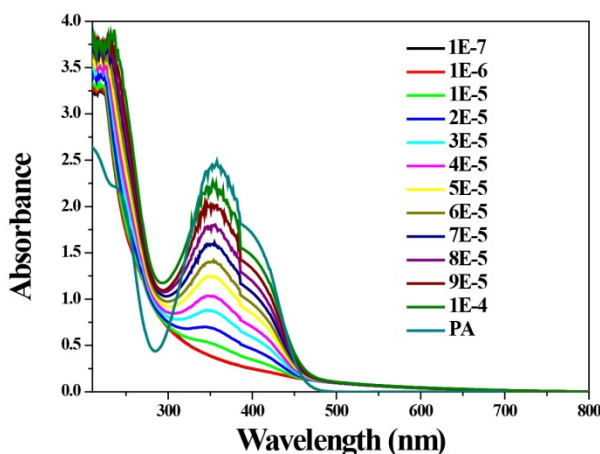


Figure S11. Mechanism of quenching depicting the overlap of absorption spectra of nitrophenols to that of OPV emission.

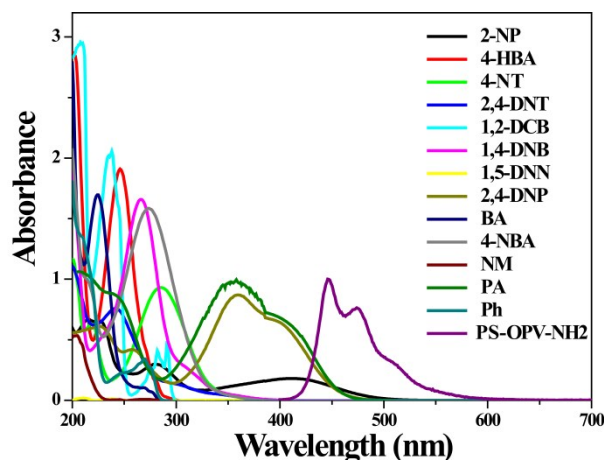


Figure S12. Emission spectra of PS-OPV-NH₂ after the addition of 1M NaCl.

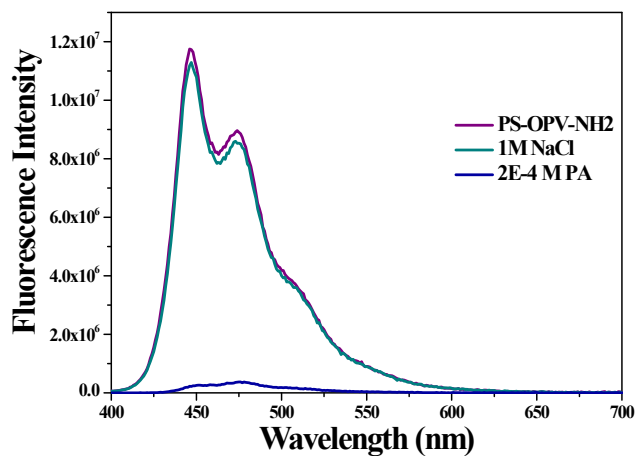
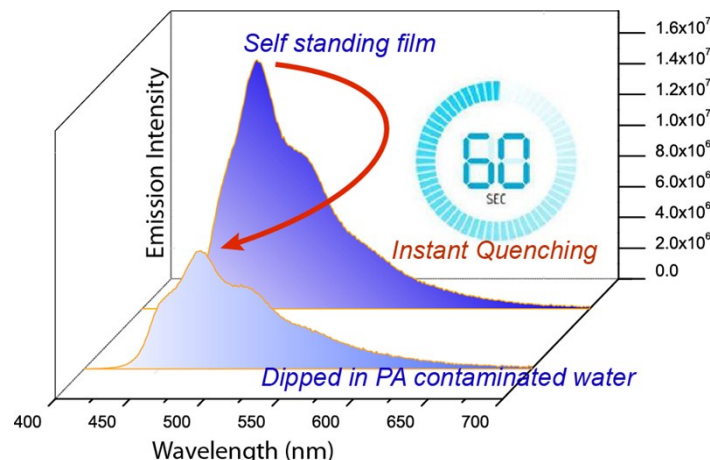


Figure S13. Quenching observed on dipping free standing film into PA in water.



References

- S1. S. S. Nagarkar, B. Joarder, A. K. Chaudhari, S. Mukherjee , S. K. Ghosh. *Angew. Chem. Int. Ed.*, 2013, **52**, 2881-2885.
- S2. K. Acharyya and P. S. Mukherjee. *Chem. Commun.*, 2014, **50**, 15788-15791.
- S3. N. Venkatramaiyah, S. Kumar and S. Patil. *Chem. Commun.*, 2012, **48**, 5007-5009.
- S4. B. Roy, A. K. Bar, B. Gole and P. S. Mukherjee. *J. Org. Chem.*, 2013, **78**, 1306-1310.
- S5. V. Bhalla, A. Gupta, M. Kumar, D. S. S. Rao , S. K. Prasad. *ACS Appl. Mater. Interfaces*, 2013, **5**, 672-679.

- S6. Z. Q. Shi, Z. J. Guo and H. G. Zheng. *Chem. Commun.*, 2015, **51**, 8300-8303.
- S7. N. Sang, C. Zhan and D. Cao. *J. Mater. Chem. A*, 2015, **3**, 92-96.
- S8. A. Ding, L. Yang, Y. Zhang, G. Zhang, L. Kong, X. Zhang, Y. Tian, X. Tao and J. Yang. *Chem. Eur. J.*, 2014, **20**, 12215-12222.
- S9. H. T. Feng and Y. S. Zheng. *Chem. Eur. J.*, 2014, **20**, 195-201.
- S10. X. G. Hou, Y. Wu, H. T. Cao, H. Z. Sun, H. B. Li, G. G. Shan and Z. M. Su. *Chem. Commun.*, 2014, **50**, 6031-6034.
- S11. W. Z. Yuan, H. Zhao, X. Y. Shen, F. Mahtab, J. W. Y. Lam, J. Z. Sun and B. Z. Tang. *Macromolecules*, 2009, **42**, 9400-9411.
- S12. P. Lu, J. W. Y. Lam, J. Liu, C. K. W. Jim, W. Yuan, C. Y. K. Chan, N. Xie, Q. Hu, K. K. L. Cheuk and B. Z. Tang. *Macromolecules*, 2011, **44**, 5977-5986.
- S13. H. Li, H. Wu, E. Zhao, J. Li, J. Z. Sun, A. Qin, and B. Z. Tang. *Macromolecules*, 2013, **46**, 3907-3914.
- S14. Y. Liu, M. Gao, J. W. Y. Lam, R. Hu and B. Z. Tang. *Macromolecules*, 2014, **47**, 4908-4919.
- S15. Y. Wang and Y. Ni. *Anal. Chem.*, 2014, **86**, 7463-7470.
- S16. S. Hussain, A. H. Malik, M. A. Afroz and P. K. Iyer. *Chem. Commun.*, 2015, **51**, 7207-7210.
- S17. D. Dinda, A. Gupta, B. K. Shaw, S. Sadhu and S. K. Saha. *ACS Appl. Mater. Interfaces*, 2014, **6**, 10722-10728.
- S18. B. Gogoi and N. Sen Sarma. *ACS Appl. Mater. Interfaces*. 2015, **7**, 11195-11202.
- S19. H. K. Sadhanala and K. K. Nanda. *J. Phys. Chem. C*. 2015, **119**, 13138-13143.
- S20. Q. Niu, K. Gao, Z. Lin and W. Wu. *Anal. Methods*. 2013, **5**, 6228-6233.
- S21. S. G. Liu, D. Luo, N. Li, W. Zhang, J. L. Lei, N. B. Li and H. Q. Luo. *ACS Appl. Mater. Interfaces*, 2016, **8**, 21700-21709.